

Synthesis and structures of calcium and strontium 2,4-di-*tert*-butylphenolates and their reactivity towards the amine co-initiated ring-opening polymerisation of *rac*-lactide

Lawrence Clark, Glen B. Deacon, Craig M. Forsyth, Peter C. Junk, Philip Mountford, Josh P. Townley, and Jun Wang

SUPPORTING INFORMATION

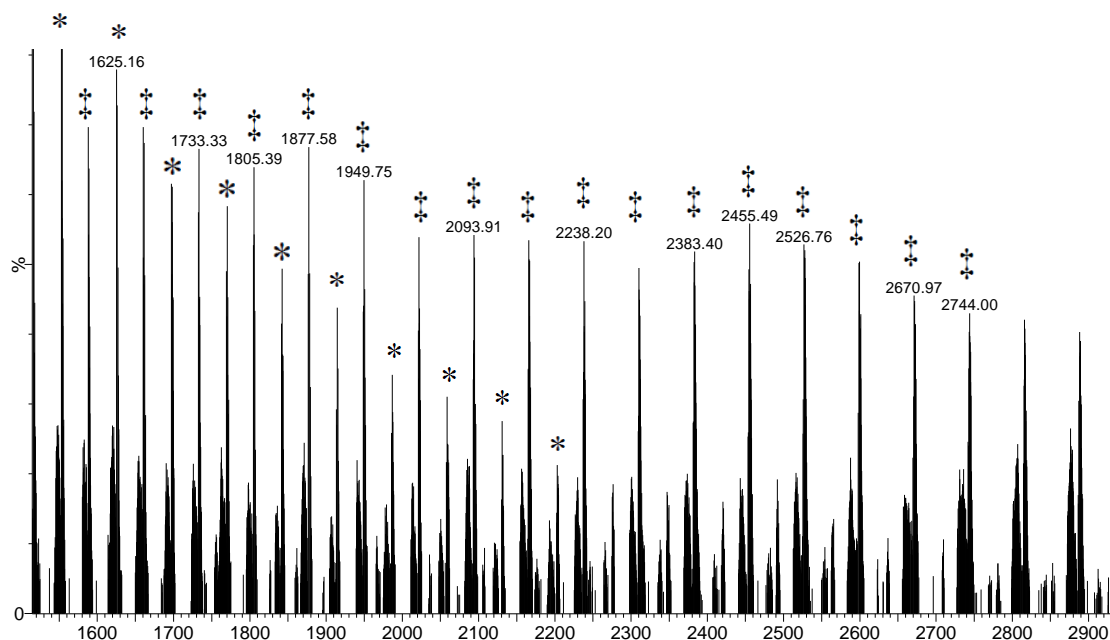


Figure S1. Representative MALDI-ToF mass spectrum of benzyl amine-capped (annotated peaks) poly(*rac*-LA) produced by $[\text{Ca}_2(\text{DBP})_4(\text{DME})_4(\mu\text{-DME})]$ (**2**) or $[\text{Sr}_2(\text{DBP})(\mu\text{-DBP})_3(\text{DME})_3]$ (**4**). Example shown is from the run with $[\textit{rac}\text{-LA}]_0:[\text{BnNH}_2]_0:[\mathbf{4}]_0 = 100:5:1$. K^+ dopant. Peak envelopes labelled “*” are for cyclic PLA ($[\text{PLA}]_n$; e.g., $m/z = 1625$ corresponds to $\{\text{K} + [\textit{rac}\text{-LA}]_{11}\}^+$). Peak envelopes labelled “‡” are for linear benzylamine-terminated PLA ($\text{H}-[\text{LA}]_n\text{-NHBn}$; e.g., $m/z = 1733$ corresponds to $\{\text{K} + \text{H}-[\textit{rac}\text{-LA}]_{11}\text{-NHBn}\}^+$). Note that $\Delta(m/z)$ between peak envelopes = 72 g mol^{-1} due to transesterification.

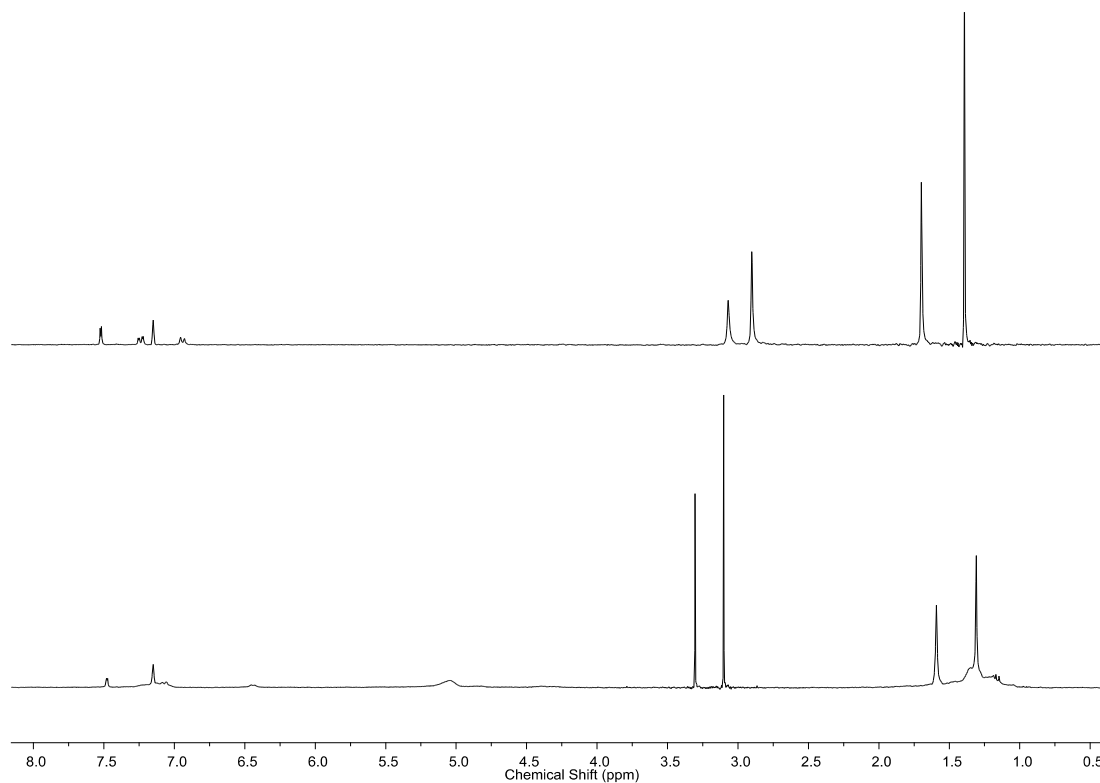


Figure S2. ^1H NMR (300.1 MHz, C_6D_6 , 298 K) spectra of $[\text{Ca}_2(\text{DBP})_4(\text{DME})_4(\mu\text{-DME})]$ (**2**) (top), and for the NMR tube scale ROP reaction with $[\text{rac-LA}]_0:[\text{BnNH}_2]_0:[\mathbf{2}] = 20:4:1$ (bottom). The signal at *ca.* 6.5 ppm in the bottom spectrum is for the NHCH_2Ph methylene group of H-[PLA]-NHBn; the broad signals between 1.1 and 1.4 ppm and at *ca.* 5.1 ppm are for the $-\text{[PLA]}-$ main chain methyl and methylene groups. Residual protio-solvent, $\delta = 7.15$ ppm.

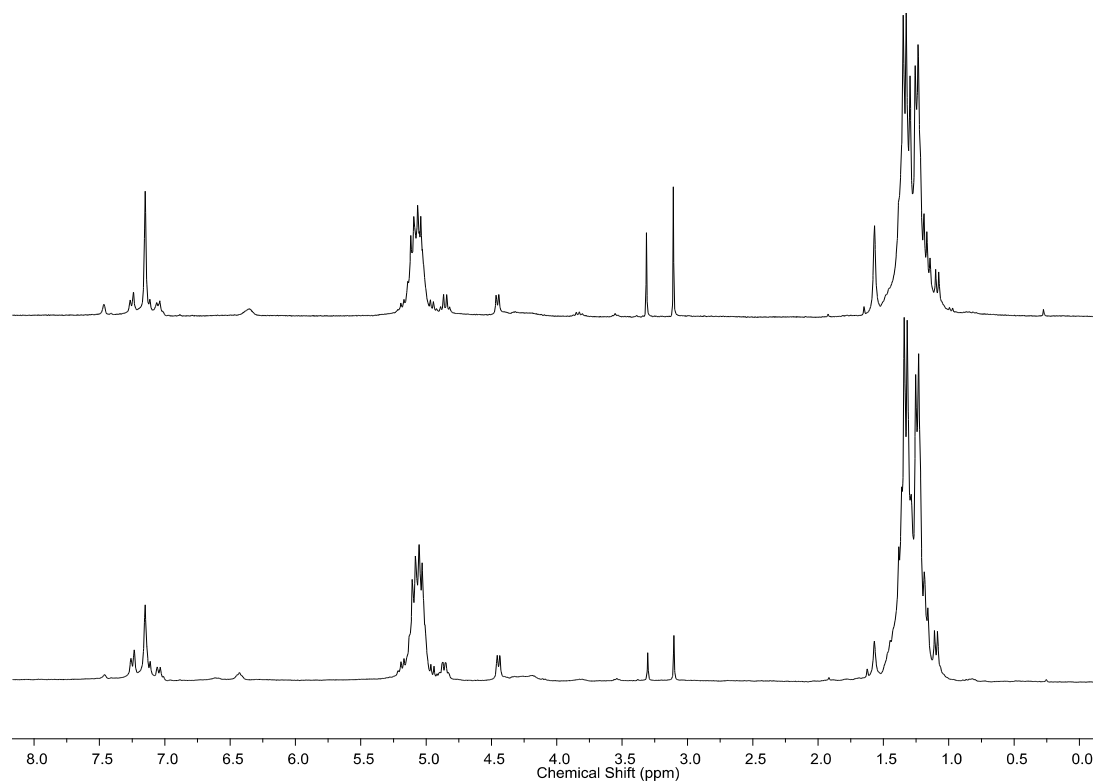


Figure S3. ¹H NMR (300.1 MHz, C₆D₆, 298 K) spectra from NMR tube scale reactions between the macromonomer H-[*rac*-LA]₁₀-NHBn and [Sr₂(DBP)(μ-DBP)₃(DME)₃] (**4**) (4:1, top), and *rac*-LA, macromonomer and **4** (20:4:1, bottom). Residual protio-solvent, δ = 7.15 ppm.

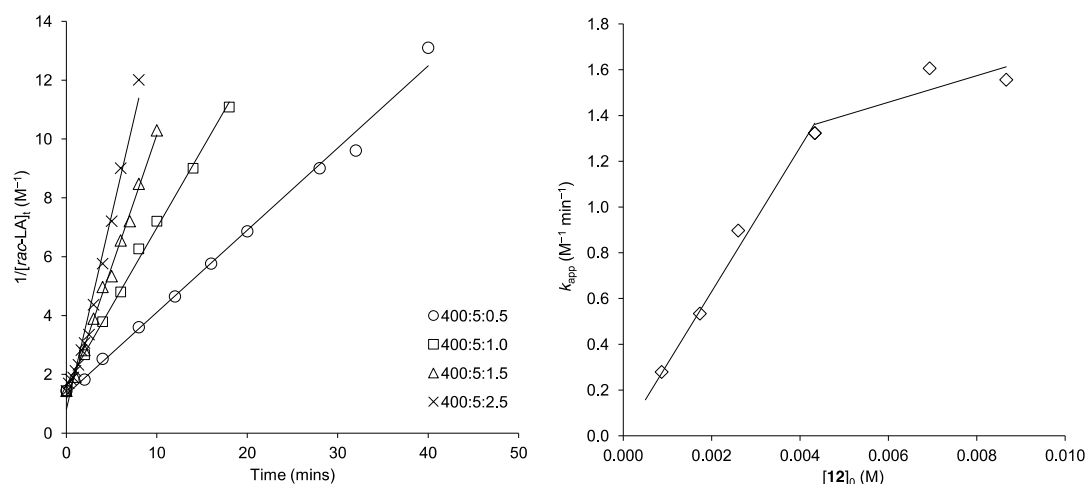


Figure S4. Left: second-order plots of $1/[\text{rac-LA}]_t$ vs. Time with increasing concentrations of $[\mathbf{2}]_0$. Rate constants, $k_{\text{app}} = 0.279(8)$ ($R^2 = 0.994$), $0.534(13)$ ($R^2 = 0.997$), $0.897(22)$ ($R^2 = 0.995$) and $1.323(52)$ ($R^2 = 0.982$) $\text{M}^{-1} \text{min}^{-1}$. The vertical-axis intercepts of the plots are $1.3(17)$, $1.64(12)$, $1.17(12)$ and $0.81(18)$ M^{-1} , (expected value = $1/[\text{rac-LA}]_0 = 1.44 \text{M}^{-1}$). Right: plots of k_{app} vs. $[\mathbf{2}]_0$. $[\text{rac-LA}]_0:[\text{BnNH}_2]_0 = 400:5$. Molar equivs. $[\mathbf{2}]_0 = 0.5-1.5$, 2.5 , 4.0 or 5.0 , $k_{p(\text{Ca})}[\text{BnNH}_2]_0^c = 315(10) \text{M}^{-2} \text{min}^{-1}$ ($R^2 = 0.987$) based on $k_{\text{app}(\text{Sr})}$ data in the range molar equivs. $[\mathbf{2}]_0 = 0.5 - 2.5$.

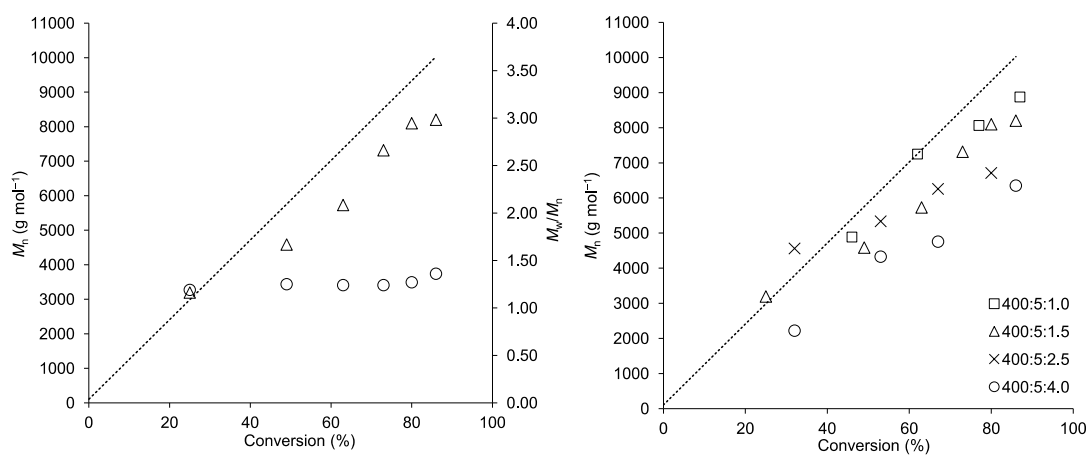


Figure S5. Left, $M_n(\text{GPC})$ vs. Conversion (triangles) and M_w/M_n vs. Conversion (circles) plots for the run $[\text{rac-LA}]_0:[\text{BnNH}_2]_0:[\mathbf{2}]_0 = 400:5:1.5$. Right, $M_n(\text{GPC})$ vs. Conversion plots with $[\text{rac-LA}]_0:[\text{BnNH}_2]_0 = 400:5$ and $[\text{rac-LA}]_0:[\mathbf{2}]_0 = 400:1.0$, 1.5 , 2.5 or 4.0 , PDIs = $1.4-1.5$. The dashed lines represent $M_n(\text{calcd})$ based on $[\text{rac-LA}]_0:[\text{BnNH}_2]_0 = 400:5$.